OPEN ACCESS

University of BRISTOL

Sarafianou, M., Gibbins, DR., Craddock, IJ., Klemm, M., Leendertz, JA., Preece, AW., & Benjamin, R. (2010). Breast surface reconstruction algorithm for a multi-static radar-based breast imaging system. In *European Conference on Antennas and Propagation (EuCAP), Barcelona, Spain* (pp. 1 - 5). Institute of Electrical and Electronics Engineers (IEEE). http://hdl.handle.net/1983/1683

Peer reviewed version

Link to publication record in Explore Bristol Research
PDF-document

University of Bristol - Explore Bristol Research
General rights

This document is made available in accordance with publisher policies. Please cite only the published version using the reference above. Full terms of use are available:
http://www.bristol.ac.uk/red/research-policy/pure/user-guides/ebr-terms/

Breast Surface Reconstruction Algorithm for a Multi-Static Radar-Based Breast Imaging System

M. Sarafianou, D.R. Gibbins, I.J. Craddock, M. Klemm, J.A. Leendertz, A. Preece and R. Benjamin

Centre for Communications Research, University of Bristol

Woodland Road, BS8 1UB, UK

M.Sarafianou@bristol.ac.uk

Abstract— **The estimation of the skin reflection is a crucial step towards successful breast tumour detection. This paper investigates the two-dimensional improved version of an existing general purpose technique for estimating target objects of arbitrary shape. The ability of the proposed method in estimating the breast skin location is tested over a wide range of realistic FDTD-based scenarios with results demonstrating accurate estimation of the breast skin location.**

I. Introduction

Breast cancer is one of the leading worldwide causes of death in women. Detecting cancer at an early stage results in a higher probability of successful treatment and will therefore reduce the mortality rates [1]. Breast cancer detection is the focus of many imaging approaches since the breast is relatively small in size and it is more physically accessible than any other internal organ [2].

X-ray mammography is currently used in the routine screening of post-menopausal women. Despite its success, it has significant risks and limitations such as high false-positive and false-negative results and unsuccessful use in pre-menopausal women due to the high density of the breast tissues [3], [4]. X-ray mammography can also be uncomfortable and there are health concerns related to exposure to ionizing radiation. This has led to the development of alternative imaging techniques, one of which is microwave breast imaging. This modality can potentially provide high-quality breast images, distinguish between healthy and malignant breast tissues and does not expose patients to ionising radiation [5].

The University of Bristol group has developed a multi-static ultra-wideband (UWB) microwave radar system for this purpose [6]. The experimental system was built in such a way so as to be used directly with real breast cancer patients and was recently used in a set of successful clinical trials. In this system, the woman lies in a prone position on an examination table, with the breast under examination in an empty part of the table, where the radar system is placed. The breast comes in direct contact with a cup, underneath which a hemispherical antenna array is located. The array consists of 31 antenna elements manufactured on separate substrates and fed by coaxial cable [6]. Figure 1 depicts the current antenna array configuration. More information regarding the array configuration can be found in [6].

Fig. 1 Top-view of the 31-element hemispherical antenna array [6]

Prior to tumour detection, the signal attributed to skin reflection must be removed so that the signal from the internal structure of the breast can be distinguished. However, before subtracting this artefact, it can also be used for the estimation of skin location. This knowledge can be valuable, particularly when applying image focusing algorithms for radar-based breast cancer detection and microwave tomography [7]. The skin location is assumed to vary among patients.

Many methods for surface estimation have been presented in the literature including not only those tailored for application to breast cancer detection [7], [8], [9] but also more general methods for other purposes, e.g. identification and rescue of wounded people in emergency cases like a fire [10], [11], [12]. The proposed algorithm takes into consideration the Envelope method presented in [12] by Kidera *et al.* The novelty of this contribution is due to two concepts: first, it considers a model of the hemispherical antenna array based on the actual antenna array configuration of the University of Bristol system. Secondly, it considers the useful data that can be extracted both from the mono-static and bi-static radar modalities. Therefore the algorithm can potentially process measured data obtained directly from the radar system.

II. PROPOSED ALGORITHM

A. System Model

This paper deals with 2-dimensional problems, by assuming a radar system that operates in both the mono-static and bi-static modes. The performance of the proposed algorithm was evaluated by applying it to data obtained using the University's in-house 3D Finite Difference Time Domain (FDTD) code.

The FDTD-based electromagnetic models consist of a surface that represents the skin layer of the breast and an antenna array in curved configuration. The breast-like phantom is considered in a pendulous position and it is assumed that the target is convex. Figure 2 depicts the configuration of the FDTD breast phantom model.

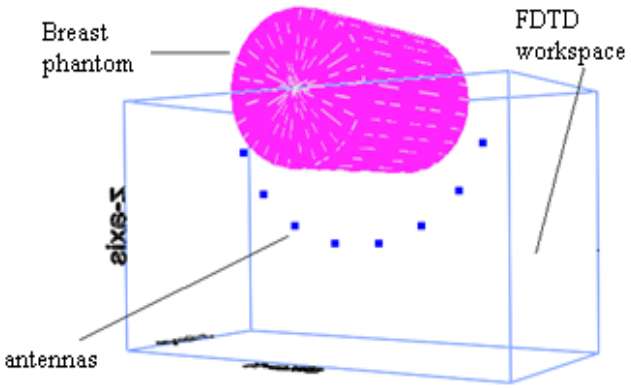

Fig. 2 3D view of the FDTD breast phantom model

FDTD breast model: In all scenarios, the breast is represented by a cylindrical phantom that has electrical properties: $\varepsilon_r = 50, \sigma = 4\text{Sm}^{-1}$. The breast phantom is immersed in a lossless medium ($\sigma = 0$) with dielectric constant equal to $\varepsilon_r = 10$. The excitation signal used is a single-cycle sinusoid with raised cosine envelope with centre frequency at 5GHz. The antenna array consists of eight point sources radiating omni-directionally in the imaging plane. The computational domain mesh is uniform with a voxel size of 0.8mm. Mur's absorbing boundary conditions (ABC) were applied.

B. 2-D Algorithm Formulation

The algorithm consists of 3 stages, which are depicted in Figure 3 and described in detail in the following sections.

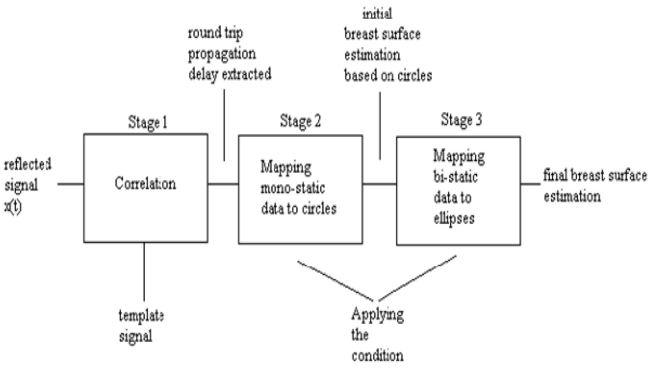

Fig. 3 Procedure overview of the novel algorithm

1) *1st Stage*: A matched filter is applied to the reflected signal in order to estimate the round trip delay. Initially, an FDTD simulation of the breast phantom model shown in Figure 2 is conducted.

The data is extracted by exciting each antenna element and recording the signals at all other antenna elements. The received signal consists of the reflected signal from the target surface (multi-path received signal) as well as other sources of clutter including the signal from the direct path between the transmitter and each receiver and reflections from the boundaries. In order to eliminate the clutter and in particular the direct path received pulse, a calibration process must be applied.

Calibration Process: The calibration process consists of three steps:

- *1st Step:* Running the FDTD simulation for the given breast phantom geometry by exciting each of the antenna elements.
- *2nd Step:* Conducting the same simulations with the phantom removed (i.e. free space).
- *3rd Step:* Subtracting the corresponding E_y field values resulting from steps 1 and 2, leading to the removal of clutter including the direct path pulse.

After extracting the calibrated reflected signals for both mono-static and bi-static problems, the round trip delay of the reflected signals must be obtained. This is achieved by "comparing" them, in other words correlating them with a reference signal (template) of known delay.

FDTD template model: To obtain the template pulse, a flat breast phantom model is considered with the same electrical properties as the breast model mentioned before. A 3D view of the template model can be observed in Figure 4. Three antenna elements, represented by point sources, are placed across the breast surface at a distance which is similar to that in the model. All simulation settings (excitation, voxel size and ABC conditions etc.) are identical to those mentioned before.

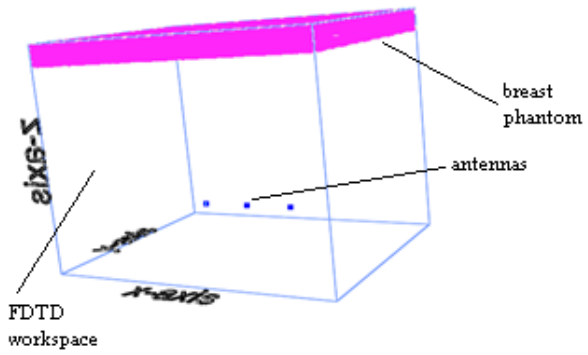

Fig. 4 Simulation environment for the FDTD template model

Correlation process: After calibrating the reflected signals from both the breast model (simulated data) and the template model, the simulated data is correlated with the template, separately for the mono-static and the bi-static problem. From this step, the round trip delay for the reflected signal is extracted.

The next processing step is the calculation of the propagation path distance from the round trip delay. This is equivalent to the distance between each antenna position and the breast surface and can be estimated from the following formula:

$$d_{rt} = \frac{c_o}{\sqrt{\varepsilon_r}} \cdot t_{rt}$$

where ε_r is the dielectric constant of the medium over which the signals propagate, c_o is the speed of light in free space and t_{rt} is the round trip delay.

2) *2nd Stage:* Considering the mono-static modality, half d_{rt} is equal to the distance between the tx antenna and the origin of the reflection. Therefore, a circle of radius $d_{rt}/2$ centred on the tx antenna, will be tangent to the surface at the point of the reflection, as depicted in Figure 5.

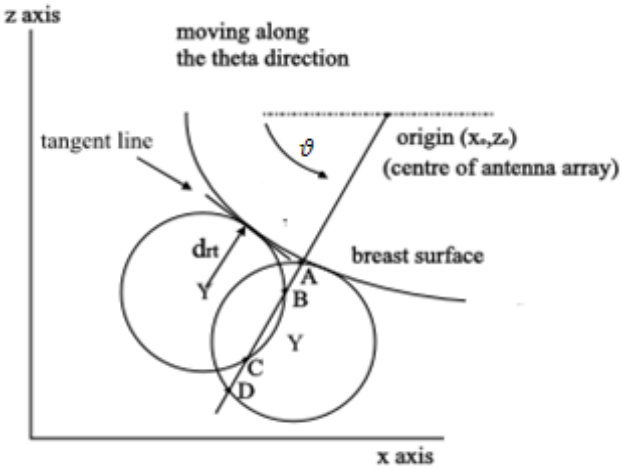

Fig. 5 Representation of the 2nd Stage (Y is the antenna position)

The boundary points that provide the breast outline are extracted from the (x, z) points of the circles that satisfy a specific condition. The condition states that the (x, z) points for a certain ϑ value, where ϑ is defined as shown in Figure 5, are chosen based on the fact that they are located at the minimum distance from the theoretical centre (origin) of the array. The coordinates (x_o, z_o) of the origin are found based on the *a priori* knowledge of all the antenna positions of the array. The condition is defined by the following formula:

$$\min_{x,z}(\,distance) = \min_{x,z}\sqrt{(x - x_0)^2 + (z - z_0)^2}$$

Better understanding of the condition can be provided through an example. As observed in Figure 5, for a certain value of ϑ, there are four possible points (A, B, C and D) that could represent the surface under construction. By applying the condition, point A is selected, since it is the closest to the origin. This is done for all the antennas in order to construct a complete surface.

3rd Stage: After the construction of the initial curve of the breast surface based on the mono-static data, the bi-static data is used to add extra information to the curve. In this case, each d_{rt} is equal to the path made by the incident signal leaving from the transmit antenna, reflected on the target surface and recorded at a receiving antenna. An ellipse can be constructed using the transmit and receiving antennas as foci and d_{rt} to construct the perimeter. Since the antenna array is in a curved configuration, the equation of the angled ellipse is extracted from its general definition as shown in Figure 6. Assume two consecutive antenna positions: transmitter (x_1, z_1) and receiver (x_2, z_2). Consider a random point on the ellipse (x, z). The distance of that point from the two ellipse foci satisfy the following equation:

$$\sqrt{(x_1 - x)^2 + (z_1 - z)^2} + \sqrt{(x_2 - x)^2 + (z_2 - z)^2} = \mathrm{d_{rt}}$$

which is the general equation of an ellipse.

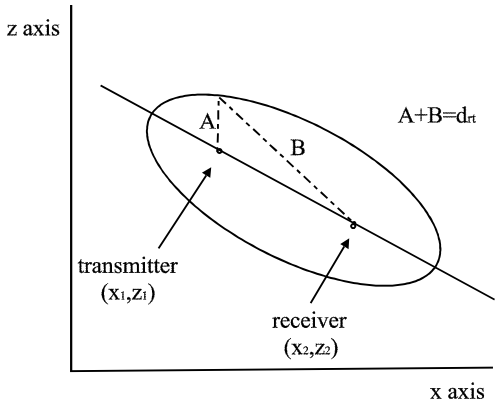

Fig. 6 Angled ellipse

In the same manner as before, for each value of ϑ, each ellipse point and the corresponding point of the reconstructed surface from the mono-static data are compared. By using the

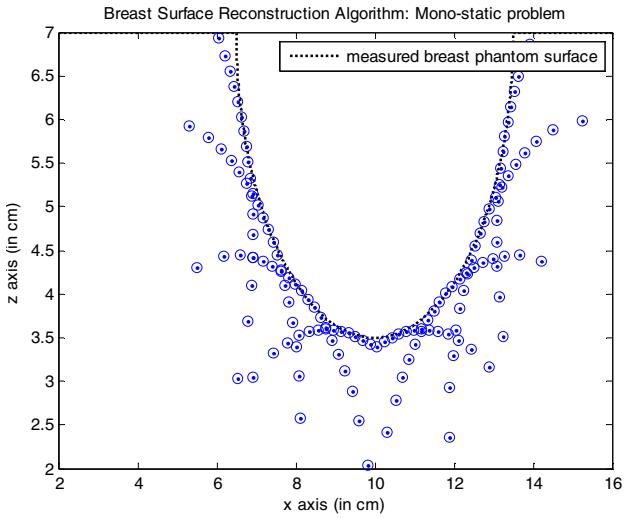

Fig. 7 Stage 2 of the reconstruction process with circles plotted as circles and the real phantom surface plotted in black

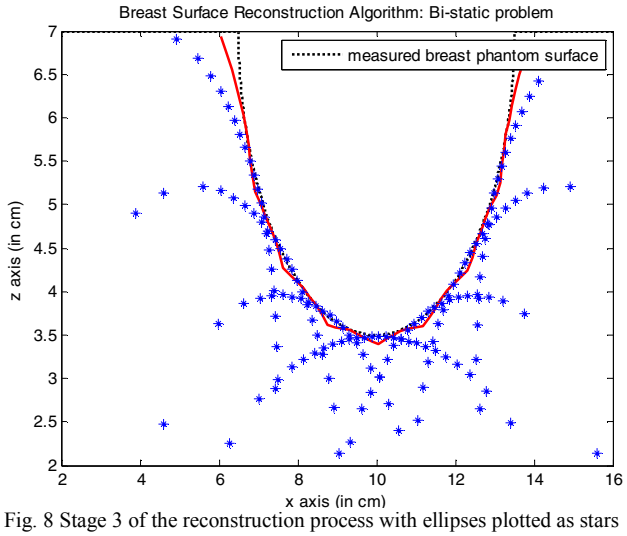

Fig. 8 Stage 3 of the reconstruction process with ellipses plotted as stars and the reconstructed surface based on circles and the real phantom surface plotted in red and black respectively

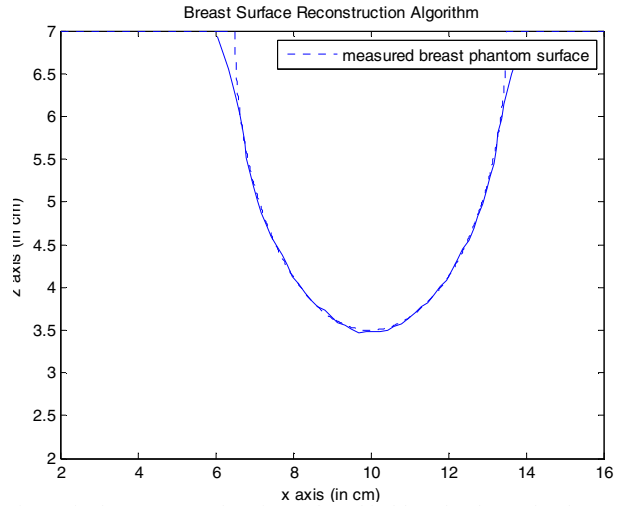

Fig. 9 Final reconstructed surface (plotted in blue) for the perfect breast phantom

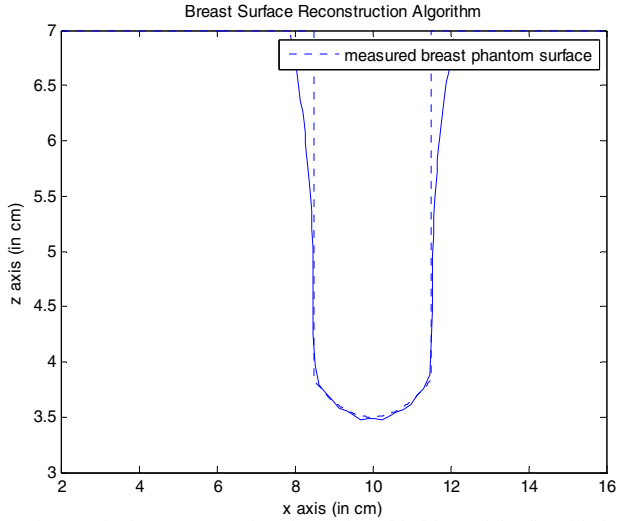

Fig. 10 Final reconstructed surface (plotted in blue) of the flat-sided phantom

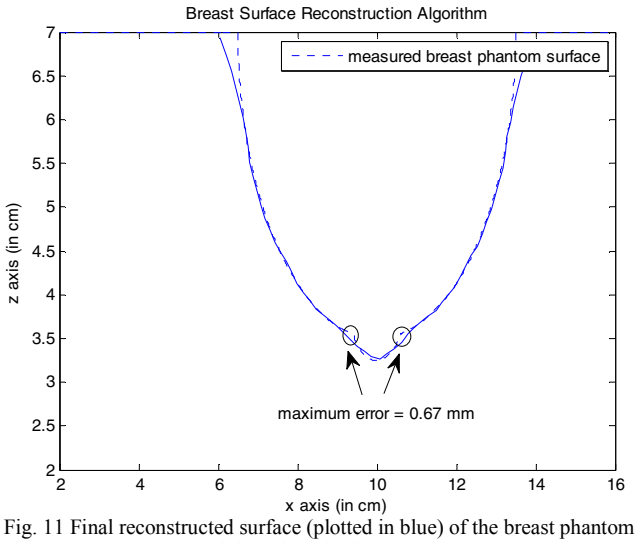

Fig. 11 Final reconstructed surface (plotted in blue) of the breast phantom with lump/nipple phantom

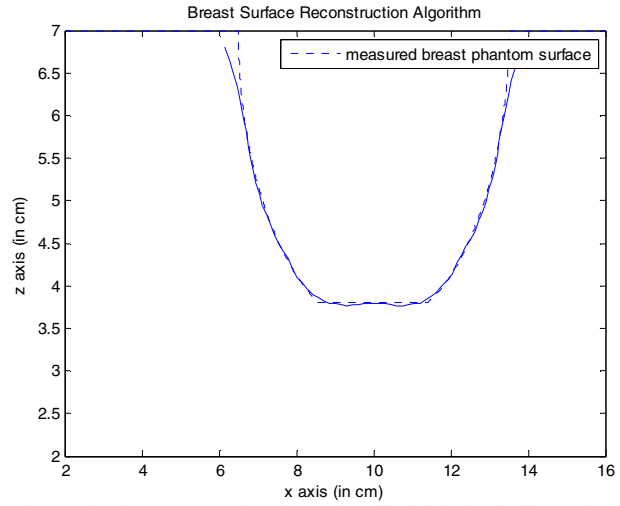

Fig. 12 Final reconstructed surface (plotted in blue) for the flat surface phantom

previously mentioned condition, the point closer to the origin of the array is chosen.

C. Algorithm Evaluation in Numerical Simulations

Four simulation scenarios were considered for the performance evaluation of the proposed algorithm.

Perfect breast phantom: Figure 7 demonstrates the circles constructed, based on the time of flight of the reflected signals recorded at the corresponding antennas. It can be seen that there are distinct parts of the circles which match the measured phantom surface.

In Figure 8, it can be observed that the breast phantom surface can be reconstructed successfully by the circles (plotted in red) but there are parts of the ellipses (plotted in stars) that can provide additional information and will further improve the reconstruction of the actual breast phantom surface. These sections of ellipses are selected through the application of the same condition and the final reconstructed surface can be seen in Figure 9.

In Figure 9, an error of less than 0.5mm in the reconstructed surface is noted. The inaccuracy observed at $x = 6.5$cm and $x = 13.5$cm is due to the lack of information at those parts of the phantom surface, since a small number of antennas are used to reconstruct the surface at that part.

Flat-sided phantom: In this case an FDTD-based distorted breast phantom model was considered. Figure 10 depicts this phantom and the final reconstructed surface. From the figure, it can be observed that the proposed algorithm provides a high degree of accuracy in the reconstruction of the breast phantom outline with an error equal to approximately 0.5mm. The error seen at the sides of the breast phantom is due to the lack of sufficient information for those parts of the phantom because of the shape and position of the array. This could be improved by adding extra antennas to the array at the sides of the phantom.

Breast phantom with lump/nipple phantom: In this scenario, a smaller cylindrical phantom was added to the perfect breast phantom geometry representing a lump or the nipple. The reconstruction of this breast model is shown in Figure 12.

As before, the breast phantom surface is accurately reconstructed with an error of less than 0.5mm. However there are two parts of the breast phantom surface (circled in Figure 11) that are reconstructed with an error of circa 0.7mm. This is because at those parts the circles are not small enough to describe that part of the surface.

Flat surface phantom: In this test case, the lower part of the breast phantom surface is flattened. Figure 12 depicts the final reconstructed surface. It can be seen that the breast phantom surface is rebuilt accurately with an error of less that 0.5mm.

D. Conclusions

This paper explored the estimation of the skin location of a breast-like phantom using a modified version of an algorithm for arbitrary surface estimation. The performance of the method was evaluated through a number of numerical scenarios.

The results indicate that the algorithm reconstructs successfully the scanned surface with an error that does not exceed 0.7mm for smooth surfaces. At the moment, work is carried out for the development of the 3D extension of the presented algorithm as well as the evaluation of its performance through simulated data and measured data obtained using the University of Bristol radar system.

ACKNOWLEDGMENT

The authors would like to acknowledge Professor J. P. McGeehan for the provision of the facilities at the Centre for Communications Research, University of Bristol and EPSRC for supporting this work.

REFERENCES

[1] Washington DC: Institute of Medicine, *Mammography and Beyond: Developing Technologies for Early Detection of Breast Cancer*, National Academy of Sciences Press, 2001.

[2] E. C. Fear, P. M. Meaney and M. A. Stuchly, "Microwaves for breast cancer detection?", IEEE *Potentials*, vol. 22, issue 1, pp. 12-18, 2003.

[3] M. L. Brown, F. Houn, E.A. Sickles, L. G. Kessler, "Screening Mammography in Community Practice: Positive Predictive Value of Abnormal Findings and Yield of Follow-up Diagnostic Procedures", *American Journal of Roentgennology*, American Roentgen Ray Society Press, vol. 165, pp. 1337-1377, 1995.

[4] P. T. Huynh, A. M. Jarolimek, S. Daye, "False Negative Mammogram", *Radiographics*, vol. 18, no. 5, pp. 1137-1154, 1998.

[5] E. C. Fear, "Microwave Imaging of the Breast", *Technology in Cancer Research and Treatment*. Vol. 4, no. 1, pp. 69-82, 2005.

[6] M. Klemm, I. J> Craddock, J. A. Leenderitz, A. Preece and R. Benjamin, "Radar-Based Breast Cancer Detection Using a Hemispherical Antenna Array- Experimental Results", *IEEE Trans. On Antennas and Propagation*, vol. 57, no. 6, pp. 1692-1704, 2009.

[7] X. Li, E. J. Bond, B. D. Van Veen and S. C. Hagness, "An Overview of the Ultra-Wideband Microwave Imaging via Space-Time Beamforming for Early-Stage Breast-Cancer Detection", *IEEE Antennas and Propagation Magazine*, vol. 47, no. 1, pp. 19-34, 2005.

[8] T. W. Williams, J. M. Sill and E. C. Fear, "Robust Approach to Skin Location Estimation for Radar-Based Breast Imaging Systems", *IEEE EMBS Conference*, Vancouver, British Columbia, Canada, pp. 5837-5841, 2008.

[9] D. W. Winters, J. D. Shea, E. L. Madsen, G. R. Frank, B. D. Van Veen and S. C. Hagness, "Estimating the Breast Surface Using UWB Microwave Monostatic Backscatter Measurements", *IEEE Trans. Biomed. Eng.*, Vol. 55, no. 1, pp. 247-255, 2008.

[10] T. Sakamoto and T. Sato, "A target shape estimation algorithm for pulse radar systems based on boundary scattering transform", *IEICE Trans. Commun.*, vol. E87-B, no. 5, pp. 1357-1365, 2004.

[11] T. Sakamoto and T. Sato, "A phase compensation algorithm for high-resolution pulse radar systems", *IEICE Trans. Commun.*, vol. E87-B, no. 6, pp. 1631-1638, 2004.

[12] S. Kidera, T. Sakamoto and T. Sato, "A Robust and Fast Imaging Algorithm with an Envelope of Circles for UWB Pulse Radars", *IEICE Trans. Commun.*, vol. E90-B, no. 7, pp. 1801-1809, 2007.

[13] D. M. Pozar, "*Microwave Engineering*", John Wiley and Sons Inc., 2005.